20th International Conference on Renewable Energies and Power Quality (ICREPQ'22)
Vigo (Spain), 27th to 29th July 2022
Renewable Energy and Power Quality Journal (RE&PQJ)
ISSN 2172-038 X, Volume No.20, September 2022

Efficient Smart Grid Fault-Identification Approach with Photovoltaic-Distributed Generators Based on Monitoring of Current/Voltage Signals

Mohamed I. Zaki[1,2], Tamer F. Megahed[1,3], and Sobhy M. Abdelkader[1,3]

[1] Egypt-Japan University of Science and Technology, Alexandria, Egypt.
Phone number:+201226055119, e-mail: **mohamed.amer@ejust.edu.eg, sobhy.abdelkader@ejust.edu.eg**
[2]Electrical Engineering Department, Faculty of Engineering, Benha University, Egypt
[3]Electrical Engineering Department, Faculty of Engineering, Mansoura University, El-Mansoura 35516, Egypt

Abstract. A Smart grid fault-identification is a critical aspect of the protection relaying system with the integration of renewable energy based on photovoltaic-distributed generators. With increasing the distributed generators usage in smart grids, the conventional relaying techniques suffer from maloperation owing to the risk of changing fault current levels. Therefore, in this paper, a discrete wavelet transform (DWT) and the statistical cross-alienation coefficients-based method is proposed to detect and classify different types of faults considering the dynamic response of photovoltaic. The proposed protection scheme does not require any extra-measuring systems as it relied on the one-ended measurements that are installed at PV-feeder over a moving window, which are available due to the use of advanced measuring facilities in smart grids. This opens the doors to transferring real-time data from / to protective relays, and then these datasets are processed for discriminating among various internal fault classes and external and healthy conditions. Intensive simulation studies are executed using PSCAD/EMTDC platform along with the validation of the proposed scheme. The 300 kW PV panel is connected to grid though a boost converter and Voltage Source Inverter. Results unveil that the application of alienation concept and differential faulty energy method for approximation coefficients-based DWT for voltage and current signals show a better performance in terms of accuracy and computational burden.

Keywords. microgrid protection, fault-identification, smart gird, renewable energy resources, photovoltaic system

1. Introduction

Future electrical grids are reliant on the development of low-greenhouse gases technologies such as Photovoltaic-Distributed Generators (PV-DGs) and wind energy to meet out the long-term climate goals that are set by implemented initiatives and regulations [1]. Also, the continuing growth in population and energy demand has promoted renewable energy production worldwide. Besides the aim of supporting primary generation and increasing system reliability and resilience, the employment of environmentally friendly generations decisively mitigates the anthropogenic emissions of carbon footprint for a sustainable future. However, the deployment of a huge number of PV-DGs in modern grids may induce new obstacles in designing fault-identification schemes owing to the soar of dynamic and bidirectional fault current. For example, an excessive PV-DGs penetration creates the mal-operation of protection equipment due to a non-linear nature of both power electronics devices and loads. Thus, the philosophy of conventional fault-identification algorithms is profoundly influenced by a penetration level, location, and operation state of PV-DGs [2].

To protect the utility grid integrated with PV-DGs, it is essential that once a fault has been made, the fault identification-based relaying system should take a fast response to detect, classify and isolate faulty phases. Here, smart relays' schemes come into the picture, which the need of fast and accurate fault identification schemes is more required to identify fault conditions so that there would be a minimum risk to the promising grid. With growing the popularity of solar energy integrated with the grid, there are extensive research works that have been proposed to develop intelligent fault identification schemes. The majority of research activities have been driven by deterministic and artificial intelligent (AI) methods [3,4]. Although the application of AI-based methods has become popular in fault detection and classification techniques, these methods require the greatest number of datasets that used for training and testing purpose. On this basis, they consume a long time to train these techniques for obtaining the accurate artificial models that can handle the dynamic nature of fault current and different grid topologies.

Recently, there has been considerable interest in fault identification-based deterministic approaches for real-time implementation of grid-connected photovoltaic [5,6,7]. For this purpose, signal processing and statistical techniques are commonly used for identifying different types of faults in smart distribution systems. In this context, there are a plethora studies, including empirical mode decomposition (EMD), Hilbert-Huang Transform (HHT), Discrete Fourier Transform (DFT), Short Time Fourier Transform (STFT), Stockwell-Transform (S-transform), Discrete Wavelet Transform (DWT), and Wavelet Packet Transform (WPT) etc.

EMD method reported in [8] have been applied to separate intrinsic mode functions (IMF) components for microgrid fault identification, but this method has a disadvantage of missing frequency information because it is reliant on time series data for signal during fault condition. HHT method and decision tree (DT) machine learning have been utilized in [9] to discriminate between faulty disturbances, switching transients, and islanding conditions. However, this

method consumes ample time due to training data through DT technique. Although the authors in [10] have introduced the fault detection and classification scheme using DFT method which processes a fault signal in frequency domain, this technique is not appropriate to analyse non-stationary signal. STFT method is presented in [11] for extracting the feature of fault signals to detect and classify different faults in distribution system. However, this method suffers from always using fixed resolution though analysis of local sections of fault signals. DWT method is proposed in [12] for a non-stationary signal to decompose fault signals in time and frequency domains, but it does not provide adequate data about a fault nature. The authors in [13] proposed a fault identification scheme using alienation coefficients for the measurement of current signal, while in [14] correlation coefficients have been used for fault detection and classification based on synchronised measurements. Despite the fact that the literature has presented different approaches for fault identification for both conventional and smart grids, the dynamic variation of fault current level and two-way power flow constitute a significant challenge. Accordingly, a fast and reliable fault identification algorithm using wavelet-based cross-alienation coefficients is proposed in this paper.

The proposed scheme must accommodate the impacts of system parameter variations due to the PV-DGs uncertainty. Based on a differential energy of Statistical Cross (X)-Alienation Coefficients (X_ACs) using low-frequency components, the improved fault identification method is designed to distinguish between internal and external fault within PV-feeder with high selectivity performance; moreover, the fault classification and faulty phase selection for all symmetrical and non-symmetrical internal faults are identified correctly.

2. Principal of the proposed methodology

The flow chart of the online fault identification application that is divided into different distinct stages is depicted in Fig. 1. As it observed, the procedure of the fault identification process is pictured in the following subsections.

A. Estimation of signal decomposition method-based DWT

In this paper, the measured voltage and current signals are captured from PSCAD/EMTDC platform, before they fed into the fault identification scheme that is implemented via MATLAB software. The measured signals are sampled with 12.8 kHz (256 samples / cycle) and the length of sliding window (1/2 cycle) which is used for signal processing and statistics purpose.

After obtaining the absolute value of the measured 3-phase voltages and currents, it is important to adopt a DWT method. The reason for this is that it is a superior multi-resolution analysis technique which can handle a non-stationary and nonlinear signal in both time and frequency domains. Therefore, this technique has ability to provide a better signal resolution at low and high frequencies. Not only detail coefficients extracted from it, but also approximate coefficients are obtained. These coefficients are extracted through the following mathematical models as formulated in Eq. (1) and Eq. (2), which convey a lot of information about signal, so many studies can use this criterion to identify fault features. However, the choice of a mother wavelet is a significant factor to perform DWT; accordingly, in this study, a db4 is adopted as a mother wavelet because it is commonly used in protection applications as in [15]. As observed, equations (1) and (2) induce approximation (CA1) and detail (CD1) coefficients at level one [16].

$$CA1[K] = \sum_{n=-\infty}^{n=\infty} X[n] * \mathrm{L}[2K-n] \tag{1}$$

$$DA1[K] = \sum_{n=-\infty}^{n=\infty} X[n] * \mathrm{h}[2K-n] \tag{2}$$

where X(n) refers to the sampled signal, and L (K) and h (K) are scaling and wavelet filters that used for decomposition process.

In this research work, the 3-phase approximation coefficients are selected to make up fault criteria with the help of cross-alienation and differential faulty energy concepts.

B. Estimation of approximate- alienation coefficients

According to the statistical analysis, the alienation of approximate coefficients that extracted from the DWT method are derived from statistical cross-correlation analysis which use to determine the degree of similarity between two sets of variables. This statistical cross (x)_correlation coefficients (X_CCs) can be expressed using the following relation [14]:

$$X\_CCs = \frac{N_s \sum y_1 * y_2 - \left(\sum y_1\right)\left(\sum y_2\right)}{\sqrt{\left[N_s \sum y_1^{\,2} - \left(\sum y_2\right)^2\right]\left[N_s \sum y_2^{\,2} - \left(\sum y_1\right)^2\right]}} \tag{3}$$

where N_s refers to the number of samples per cycle, (N_s= 256 samples/ cycle considering sampling frequency 12.8 kHz. y_1 represents sampled voltage or current approximate coefficients at time t_0 (current window), while y_2 is sampled voltage or current approximate coefficients at time —— T -+ t_0 (previous window).

As mentioned before, X-alienation coefficients are calculated from X-correlation coefficients, which can be formulated as follow [13]:

$$X\_\mathrm{A}Cs = 1 - X\_CCs^2 \tag{4}$$

After computing Approximate-Alienation Coefficients (AACs), these coefficients are exploited to make a fault identification index that is invented to identify faulty cases in the utility grid integrated with the intermittent PV-feeder.

C. *Estimation of fault-identification index*

A Fault-Identification Index (F-II) is constituted by computing the peak value of differential faulty energy for 3-phase AACs through the moving window technique using the following proposed mathematical expression:

$$F\_II = \max\left(\frac{\left[AACs^2(\mathrm{t}) - \min\left(AACs^2(\mathrm{t})\right)\right]}{\left[\max\left(AACs^2(\mathrm{t})\right) - \min\left(AACs^2(\mathrm{t})\right)\right]}\right) \tag{5}$$

where min and max refer to the minimum and maximum values, respectively.

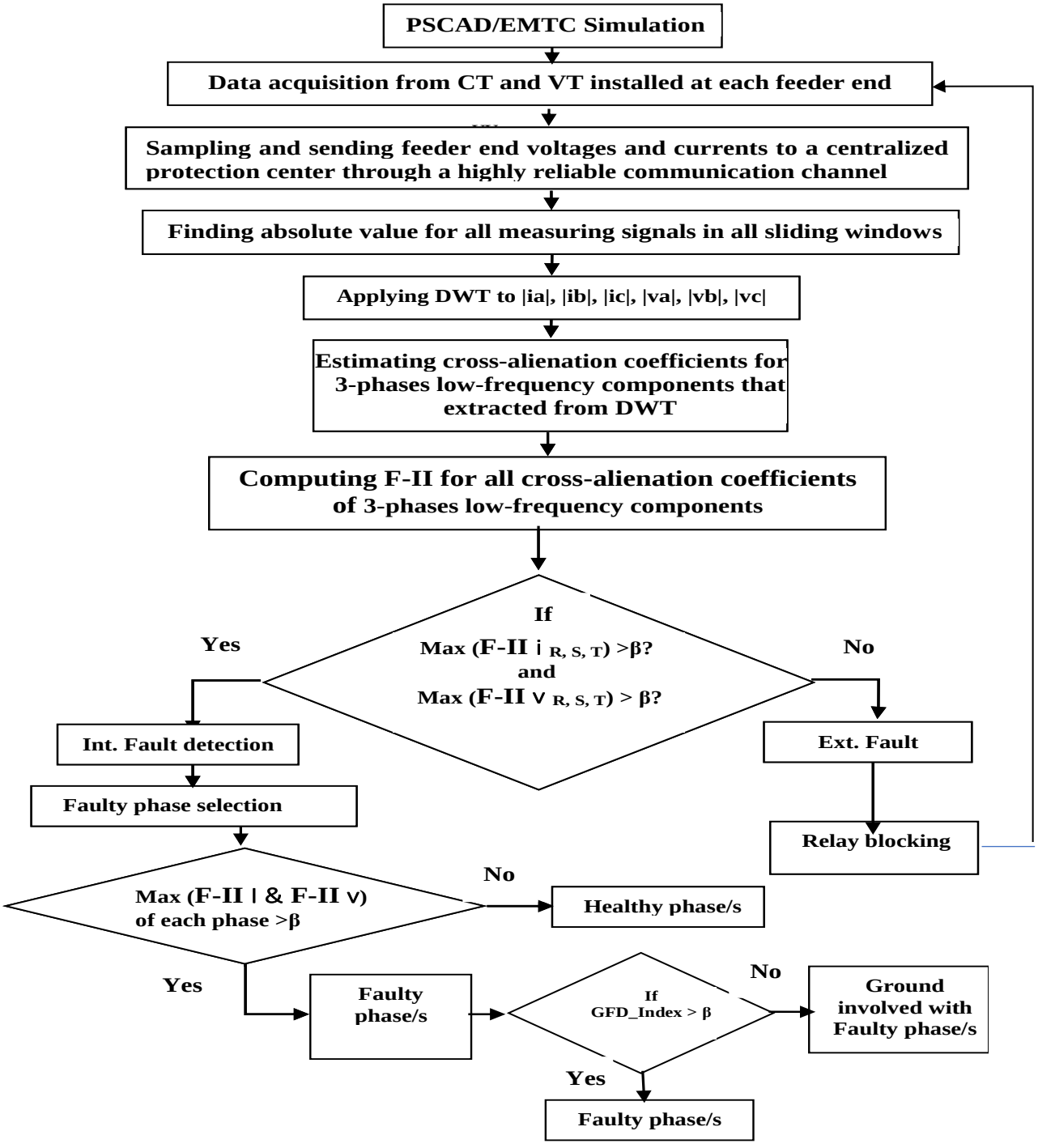

Fig. 1. The flow chart of the proposed fault identification scheme

A threshold value of 0.1 is set to figure out faulty and non-faulty phases. If the peak amplitude value of *F_II* corresponding to a phase is greater than the determined threshold value and close to unity, then faulty phases are declared, else other phases are healthy in nature. The value of 0.1 is considered as a threshold for *F_II* in order to make the differentiation of faulty phases from health ones. This value is chosen based on a 200-datasets of every fault. As a result, a 1000 set of data has been considered for all fault kinds. This data is captured by varying fault and system parameters, such as fault type, fault resistance, fault location, bidirectional power flow, feeder energization and de-energization, and load switching. Also, those associated with varying irradiance and temperature of PV array integrated with the grid is considered. It is evident that the value of 0.1 is effective to discreminate fault condition for all possibilites of fault scenarios that is more likely to occur in the grid integrated with PV array panel.

D. *Estimation of ground fault-detection index*

A ground fault detection (GFD)-index is proposed to recognise the fault scenario that involves zero sequence current, by which is used to identify grounded faults, like a 1-phase to ground fault and a 2-phase to ground fault. The GFD-index is reliant on the computation of zero sequence current (I_{ZSC}) that flow while grounded fault occurrence, which can be expressed as following relation [17]:

$$I_{ZSC} = \frac{I_R + I_S + I_T}{3} \tag{6}$$

Using the decomposition of DWT method, the approximation coefficients of I_{ZSC} is computed. Having obtained these coefficients, the differential faulty energy corresponding to the approximation coefficients of I_{ZSC} is applied, and it can be expressed as in (7) to differentiate the ground faults.

$$GFD\_Index = max\left(\frac{\left[A^2_{ZSC}(t) - min\left(A^2_{ZSC}(t) \right) \right]}{\left[max\left(A^2_{ZSC}(t) \right) - min\left(A^2_{ZSC}(t) \right) \right]} \right) \tag{7}$$

where A_{ZSC} is the approximation coefficients for I_{ZSC}.
Based on the value of GFD_index, if it is close to unity, this indicate to a 1- phase to ground fault or a 2-phase to ground fault, else the value indicates that the involvement of ground in the fault is not found.

3. Applications

A. *Description of simulation model for electrical grid integrated with PV-feeder*

The proposed algorithm has been successfully tested on the studied grid as illustrated in Fig. 2, which consists of solar photovoltaic (PV) power plant. The 300 kW PV panel is connected to grid though a DC/DC boost converter, DC/AC Voltage Source Inverter (VSI). After inversion, the PV-system is linked to the distribution system through 0.6/20 kV transformer and transmission line (TL1) of 10 Km length. The 20 kV-grid is interfaced to 230 KV through two transmission lines (TL_2 and TL_3), each of which has length 20 km, and a 100 MVA, 20 kV /230 kV power transformer. All the data pertaining to transformers, feeders, PV-system, and loads are obtained from [18]. The studied power system is simulated via PSCAD/EMTDC platform, and different fault parameters and operation condition are carried out through this platform to investigate the performance of the proposed scheme.

B. *Simulation results*

Taking the signal length of 3 seconds for simulation run with operating frequency 50 Hz, the voltages and currents that are measured by an installed relay at the PV-feeder are sampled at 12.8 kHz (256 samples / cycle). Once a half-cycle movable window is selected, its samples are sorted (current window) and compared with the previous one. The half-cycle window width (128 samples) has been considered for calculating the proposed *F_II* based on approximation-alienation coefficients for both voltage and current signals. The proposed *F_II* and GFD_criteria are estimated using the measured sampled signals within a current window and an earlier one to show the degree of variance of two sets of data. To validate the robustness of the proposed fault identification algorithm, all fault classes (i.e., symmetrical, and non-symmetrical faults) have been simulated at 2s with the fault duration 1s for both a distribution system level and a PV-feeder. In addition to this, the variation of fault parameters (i.e., fault locations and fault resistances) has been considered.

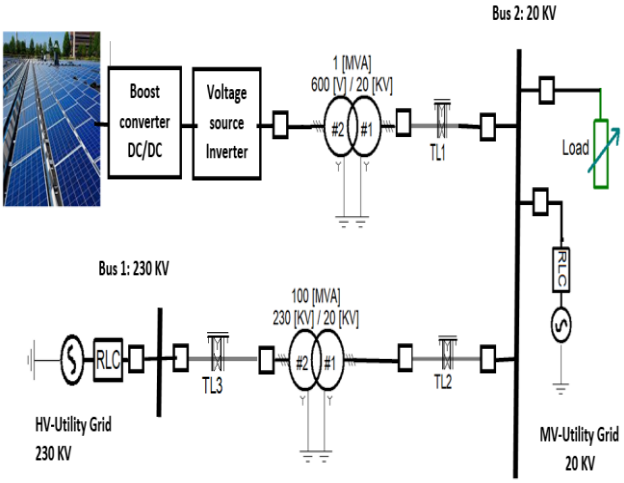

Fig.2 Single line diagram of smart distribution network integrated with PV-DG

4. Results and Performance-Evaluation

A. *Influence of internal fault under grid-connected mode*

The transients that are induced due to the post fault current and voltages are largely reliant on a fault type. Thus, it is necessary to test the proposed fault identification scheme for different fault types. In this study, different kinds of faults have been simulated at a midpoint of line TL1 (PV-feeder), with fault resistance (3Ω). Fig.3. depicts the variation of fault-identification indices of three phase voltage and currents with a phase to ground fault.in phase R. From Fig.3. (b) and Fig.3. (d), it is clear that the fault index of phase-R is always close to unity and exceeds threshold β-value compared to the *F-II v, I* for remained phases. Therefore, it is identified as a phase to ground fault in Phase R.

As the same way, Fig.4 shows the *F-II* of phase-R and phase-S for both voltage and current signals are above threshold β-value. In addition to this, the GFD-index is also determined and equals 0.8 corresponding to (7) based on calculating I_{ZSC} that follow through system during one phase to ground fault and two-phase to ground fault. Thus, this fault identified as a two-phase to ground fault in a phase-R and a phase-S.

Similarly, From Fig.5, it can be observed that, for all three phases R, S, T the *F-IIs* of voltage and current are close to unity and greater than threshold β-value, and the GFD-index is determined as 0.03, which is near to zero. Hence, this fault identified as a three-phase to ground fault in a phase-R, phase-S, and phase-T. Therefore, the proposed scheme is insensitive to different fault types that have been occurred in PV-feeder which is connected to medium voltage grid.

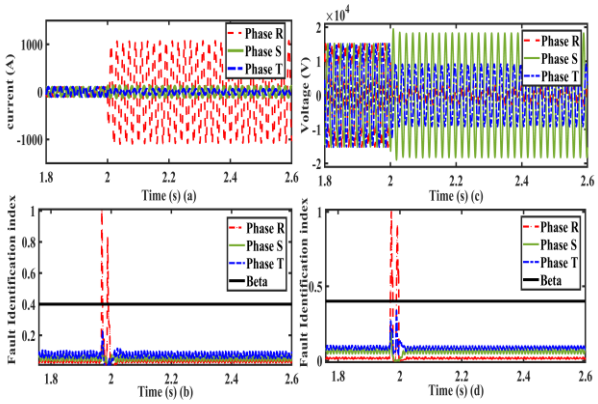

Fig. 3. *Phase R to ground fault at TL1 with 3 Ω fault resistance: (a) current waveform; (b) the variation of fault identification index of measured current at PV-feeder during the fault; (c) voltage waveform; (d) the variation of fault identification index of measured voltage at PV-feeder during the fault.*

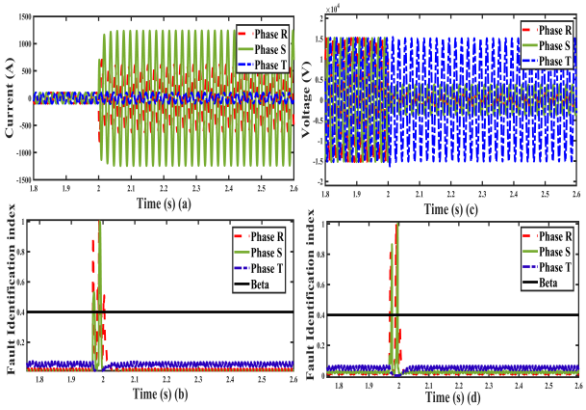

Fig. 4. Double phase to ground fault in phases R and S at TL1 with 3 Ω fault resistance: (a) current waveform; (b) the variation of fault identification index of measured current at PV-feeder during the fault; (c) voltage waveform; (d) the variation of fault identification index of measured voltage at PV-feeder during the fault.

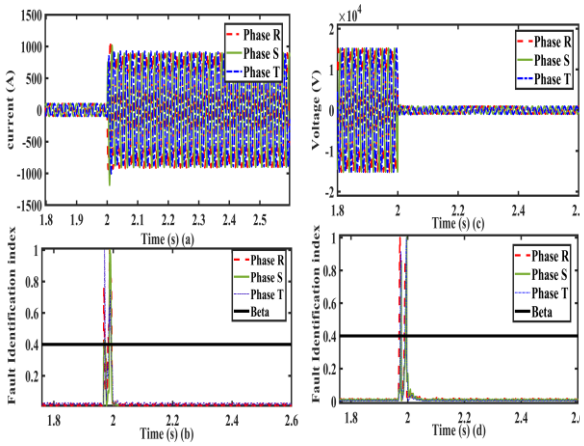

Fig. 5. Triple phase to ground fault in phases R, S, and T at TL1 with 3 Ω fault resistance: (a) current waveform; (b) the variation of fault identification index of measured current at PV-feeder during the fault; (c) voltage waveform; (d) the variation of fault identification index of measured voltage at PV-feeder during the fault.

B. flexibility of the proposed scheme against varying fault resistance

The post fault voltage and current are highly reliant on a fault location and resistance. Thus, it is important to verify the proposed fault identification scheme for different fault locations and resistances. In this work, different kinds of faults have been simulated at a midpoint of line TL1 (PV-feeder), with a wide range of fault resistance from 0.1 Ω to 80 Ω. As listed in Table 1, the variation of fault-identification indices of three phase voltage and currents under different fault resistances and types for faulted phase/s are near to one and greater than threshold βvalue, which indicates that a fault occurred in these phases within PV-feeder. Consequently, the proposed scheme would not be mal-function due to the variation of fault resistance.

C. Influence of external fault under grid-connected mode

Table 1 The performance of the proposed c scheme under various internal and external faults with different fault parameters

Fault type	RF (Ω)	Fault location	Fault-Identification Index						(GFD)-index	Final Relay Decision
			F-IIi $_R$	*F-IIi* $_S$	*F-IIi* $_T$	*F-IIv* $_R$	*F-IIv* $_S$	*F-IIv* $_T$		
Healthy	---	------	0.061	0.082	0.046	0..052	0.076	0.046	0	
PGF	10	50% of TL_1	**0.97**	0.308	0.19	**0.99**	0.125	0.06	**0.960**	**Tripping** for Int. AG fault
PPGF	20	50% of TL_1	**0.87**	**0.98**	0.18	**1**	**0.998**	0.06	**0.934**	**Tripping** for Int. ABG fault
PP	25	50% of TL_1	**0.93**	**0.97**	0.1	**0.89**	**0.92**	0.09	**0**	**Tripping** for Int. AB fault
PPPG	50	50% of TL_1	**0.84**	**0.95**	**0.81**	**1**	**1**	**0.99**	**0**	**Tripping** for Int. ABCG fault
PGF	5	50% of TL_2	0.368	0.3	0.31	0.616	0.231	0.336	0.754	**Blocking** for Ext, fault
PPGF	15	50% of TL_2	0.286	0.32	0.212	0.718	0.398	0.039	0.810	**Blocking** for Ext, fault
PPF	60	50% of TL_2	0.544	0.316	0.146	0.263	0.237	0.103	0	**Blocking** for Ext, fault
PPPGF	30	50% of TL_2	0.268	0.418	0.252	0.318	0.239	0.514	0	**Blocking** for Ext, fault
PGF	40	50% of TL_3	0.148	0.135	0.166	0.219	0.09	0.07	0.674	**Blocking** for Ext, fault
PPGF	12	50% of TL_3	0.049	0.178	0.164	0.112	0.098	0.706	0.78	**Blocking** for Ext, fault
PPF	1	50% of TL_3	0.269	0.189	0.155	0.218	0.217	0.119	0	**Blocking** for Ext, fault
PPPGF	0.1	50% of TL_3	0.232	0.370	0.251	0.297	0.228	0.349	0	**Blocking** for Ext, fault
PGF	80	Bus 2	0.273	0.101	0.112	0.201	0.084	0.754	0.642	**Blocking** for Ext, fault
PPGF	6	Bus 2	0.171	0.252	0.104	0.116	0.321	0.338.	0.632	**Blocking** for Ext, fault
PPF	35	Bus 2	0.155	0.288	0.109	0.168	0.172	0.129	0	**Blocking** for Ext, fault
PPPG	45	Bus 2	0.201	0.103	0.276	0.038	0.128	0.135	0	**Blocking** for Ext, fault

- Int. fault: Internal fault
- Ext fault: External fault

The proposed fault identification scheme was investigated under different external fault scenarios within a MV /HV grid that integrated with the PV-feeder (see Fig. 2). Simulation results are described in Table 1. Taking a phase to ground fault in phase-R at the middle of TL2 line, as example, the *F-II* of faulty phase for both voltage and current waveform is not close to unity ($F\text{-}II_{iR}$ **=0.368**, $F\text{-}II_{vR}$ **=0.616)** and one of them is less than the threshold β-value ($F\text{-}II_{iR}$ **=0.368 <β,** $F\text{-}II_{vR}$ **=0.616>β).** According to the proposed fault identification scheme, these results indicate to finding external fault, compared with the healthy case of the power system test, the values of F-II for the measured signals at the PV-feeder are very close to zero ($F\text{-}II_{iR=}$ **0.061**, $F\text{-}II_{iS=}$ **0.082**, $F\text{-}II_{iT=}$**0.046**, $F\text{-}II_{vR=}$ **=0.052**, $F\text{-}II_{vS=}$**0.076**, $F\text{-}II_{vT}$**=0.046**). Therefore, the possibility of identifying external fault conditions from internal faults is illustrated in Table 1, and it is evident that the proposed scheme has a superiority to discriminate between internal and external faults. Furthermore, different external fault scenarios that are carried out on midpoint of TL3 line and bus 2 show the capability of proposed scheme to recognise the external fault condition from internal one within PV-feeder. Thus, from Table 1, it can be concluded that in the case of external fault with varying fault parameters, the behaviour of *F-II* for all phases is completely different from the case of internal fault, and therefore an external fault is not affected in the proposed scheme compared to existing schemes that are reported in the literatures.

5. Conclusions

Based on the usage of approximation-alienation coefficients for both voltage and current signals, this paper presents an effective fault identification scheme for a smart grid integrated with PV-system through the available power electronics facilities. An accurate, efficient, and fast fault identification scheme has introduced considering the dynamic fault current response for the grid interfaced with PV-system. In this scheme, once the DWT is employed to extract the approximation components for measured signals, cross alienation coefficients are computed based on these approximation components. Then, the differential faulty energy is calculated and defined as a fault identification index that is used to discriminate between internal and external fault. The simulation results reveal that the fault identification scheme can differentiate between internal and external fault with high selectivity performance. Moreover, after internal fault is declared, the scheme can classify the fault type and select the faulty phase within half cycle moving window.

Acknowledgements

The authors are grateful to Prof. Tanemasa Asano of Kyushu University for his useful comments on this work.

References

[1] N.Y. Amponsah, M. Troldborg, B. Kington, I. Aalders, R.L. Hough, Greenhouse gas emissions from renewable energy sources: a review of lifecycle considerations, Renew. Sustain. Energy Rev. 39 (2014) 461e475.

[2] Jiang, H., Dai, X., Gao, D. W., Zhang, J. J., Zhang, Y., & Muljadi, E. (2016). Spatial-temporal synchrophasor data characterization and analytics in smart grid fault detection, identification, and impact causal analysis. IEEE Transactions on Smart Grid, 7(5), 2525-2536.

[3] Adhya, D., Chatterjee, S., & Chakraborty, A. K. (2022). Performance assessment of selective machine learning techniques for improved PV array fault diagnosis. Sustainable Energy, Grids and Networks, 29, 100582

[4] Gupta, N., Seethalekshmi, K., & Datta, S. S. (2021). Wavelet based real-time monitoring of electrical signals in Distributed Generation (DG) integrated system. Engineering Science and Technology, an International Journal, 24(1), 218-228.

[5] da Costa Pinho, A., & Garcia, E. G. A. (2022). Wavelet spectral analysis and attribute ranking applied to automatic classification of power quality disturbances. *Electric Power Systems Research*, *206*, 107827.

[6] Sampaio, F. C., Leão, R. P., Sampaio, R. F., Melo, L. S., & Barroso, G. C. (2020). A multi-agent-based integrated self-healing and adaptive protection system for power distribution systems with distributed generation. *Electric Power Systems Research*, *188*, 106525

[7] Chabanloo, R. M., Maleki, M. G., Agah, S. M. M., & Habashi, E. M. (2018). Comprehensive coordination of radial distribution network protection in the presence of synchronous distributed generation using fault current limiter. *International Journal of Electrical Power & Energy Systems*, *99*, 214-224.

[8] Roy, Gargi, Soyel Ghosh, and Arpendra Roy. "A Novel Approach to Microgrid Fault Detection Using Empirical Mode Decomposition." Applications of Networks, Sensors and Autonomous Systems Analytics. Springer, Singapore, 2022. 103-111.

[9] Shaik, Mahmood, Abdul Gafoor Shaik, and Sandeep Kumar Yadav. "Hilbert-Huang transform and decision tree-based islanding and fault recognition in renewable energy penetrated distribution system." Sustainable Energy, Grids and Networks (2022): 100606.

[10] Prasad, C. D., & Nayak, P. K. (2019). A DFT-ED based approach for detection and classification of faults in electric power transmission networks. *Ain Shams Engineering Journal*, *10*(1), 171-178.

[11] Ukil, A., Yeap, Y. M., & Satpathi, K. (2020). Frequency-domain based fault detection: Application of short-time fourier transform. In *Fault Analysis and Protection System Design for DC Grids* (pp. 195-221). Springer, Singapore.

[12] Zaki, M. I., El Sehiemy, R. A., Amer, G. M., & El Enin, F. M. A. (2019). Sensitive/stable complementary fault identification scheme for overhead transmission lines. *IET Generation, Transmission & Distribution*, *13*(15), 3252-3263.

[13] Mahfouz, M. M., & El-Sayed, M. A. (2016). Smart grid fault detection and classification with multi-distributed generation based on current signals approach. *IET Generation, Transmission & Distribution*, *10*(16), 4040-4047.

[14] Chatterjee, B., & Debnath, S. (2020). Cross correlation aided fuzzy based relaying scheme for fault classification in transmission lines. *Engineering Science and Technology, an International Journal*, *23*(3), 534-543.

[15] Zaki, M. I., El-Sehiemy, R. A., & Amer, G. M. (2021). Efficient fault identification scheme of compensated transmission grid based on correlated reactive power measurements and discrete wavelet transform. *Journal of Electrical Engineering*, *72*(4), 217-228.

[16] Zaki, M. I., El-Sehiemy, R. A., Amer, G. M., & El Enin, F. M. A. (2019). An investigated reactive power measurements-based fault-identification scheme for teed transmission lines. *Measurement*, *136*, 185-200.

[17] Zaki, M. I., El Sehiemy, R. A., Amer, G. M., & El Enin, F. M. A. (2017, December). Integrated discrete wavelet transform-based faulted phase identification for multi-terminals power systems. In *2017 Nineteenth International Middle East Power Systems Conference (MEPCON)* (pp. 503-509). IEEE.

[18] Ndjakomo Essiane, S., Gnetchejo, P. J., Ele, P., & Chen, Z. (2021). Faults detection and identification in PV array using kernel principal components analysis. *International Journal of Energy and Environmental Engineering*, 1-26.